

The Influence of Infection Control Policies: A Systematic Study of the Dynamics of an Individual-based Epidemic Model with Isolation

Andreas Reppas, Andreas C. Tsoumanis, Constantinos I. Siettos

Abstract—We present and discuss how the so called Equation-free approach for multi-scale computations can be used to systematically study certain aspects of the dynamics of detailed individual-based epidemic simulators. In particular we address the development of a computational protocol that enables detailed epidemic simulators to converge to their coarse-grained critical points which mark the onset of instabilities including the emergence of time-dependent solutions. As our illustrative example, we choose a simple individual-based stochastic epidemic model deploying in a fixed random regular network. We show how control policies based on the isolation of the infected population can dramatically influence the dynamics of the disease resulting to big-amplitude oscillations. We also construct the approximate coarse-grained bifurcation diagrams illustrating the dependence of the solutions on the disease characteristics.

I. INTRODUCTION

THE quest for the efficient modeling, analysis, long-term prediction and control of infectious disease spread is one of the most significant and tough research pursuits of our time.

Towards this aim, a variety of public-health measures and policies have been proposed in order to control the outbreak of a disease in an efficient way. The ultimate goal is the design and the development of prevention policies to help control or even extinguish a possible epidemic or even pandemic threat.

One of the most common strategies is vaccination of targeted population [1], [2]. Another health measure which has been historically used in the control epidemics concerns the special treatment –quarantine or isolation– of the infected part of the population [3]. In the study of [3]–[5] it has been shown that such a strategy may result to the eradication of the epidemic. The public intervention of isolation and quarantine has also been used in [6], [7] along with clinical data to express the efficiency of those measures in diseases such as SARS, Smallpox, Pandemic Influenza and HIV.

There is no doubt that mathematical models and systems theory are playing a most valuable role in shedding light on

the problem and helping make decisions. A large and intensive research effort is evolving for the development of better and more detailed models including expertise from inter-disciplinary fields ranging from molecular biology and epidemiology to sociology and applied mathematics. The studies have proceeded mainly on two main directions. On the one hand, there are the “continuum models” in the form ordinary or partial-integral-differential equations [8], [9]. However, due to the complexity of the phenomena, available continuum models are often qualitative caricatures of the reality. On the other hand, there are the so-called object-based models where the problem is modeled as a network of interacting discrete entities (or as otherwise called individuals, components or objects). These models include detailed information of the spreading mechanisms such as the structure of the social network, the mobility and the everyday interactions of each individual, demographics of age and income as well as knowledge in the molecular/virus level [10]–[12].

However a fundamental prerequisite for the systematic analysis of the dynamics and the design of control processes is the availability of reasonably accurate closed-form dynamical models. Yet, for object-based epidemic models, due to their inherent complexity, the closures required to formulate representative continuum models are not usually available. When this is the case, conventional continuum algorithms cannot be used directly for systematic systems level analysis and control-intervention policies design.

In current practice, what is done with these detailed individual-scaled epidemic simulators is simple time-integration: set-up many initial conditions to span the phase space, for each initial condition create a large enough number of ensemble realizations, probably change some of the rules and then run the detailed dynamics for a long time to investigate how things such as different vaccination policies and malignancy of the virus may influence the spread of an outbreak.

However, this “simple” simulation is inadequate for systematic analysis of the emergent coarse-grained dynamics and consequently for control design purposes. For example important tasks such as the efficient exact location of the critical points that mark the onset of outbreaks and other phenomena such as undesirable big-amplitude epidemic oscillations cannot be easily obtained through just temporal simulations.

In this work we show how the so-called Equation-free approach for multi-scale computations [13]–[18] can enable detailed epidemiological simulators to converge to their coarse-grained criticalities. In particular we address a

Manuscript received August 5, 2008. This work was supported in part by the National Technical University of Athens through the Basic Research Program “Constantin Caratheodory”.

A. Reppas is with the School of Applied Mathematics and Physical Sciences, National Technical University of Athens.

A. B. Tsoumanis, is with the School of Chemical Engineering, National Technical University of Athens.

C. I. Siettos is with the School of Applied Mathematics and Physical Sciences, National Technical University of Athens (phone: +30 210 7723950, fax: +30 210 7721302; e-mail: ksiet@mail.ntua.gr).

computational framework under which one can detect coarse-grained bifurcations such as Neimark-Sacker criticalities that mark the onset of periodic solutions. This is achieved by treating the epidemic simulator as a black-box input-output map of the coarse-grained variables, by-passing the derivation of closed-form continuum models.

For our illustrations we develop and use an individual-based epidemic model with nonlinear incidence rates where individuals interact in a caricature of a social network approximated by a random regular graph. We describe the rules governing the evolution of the individuals health- state dynamics and investigate how the control policy, that is the way that infected individuals are held isolated until they recover, can affect drastically the dynamics of the spreading leading to coarse-grained nonlinear phenomena such as the emergence of sustained oscillations, i.e., boom and bust disease outbreaks.

The paper is organized as follows: in section two we present the individual-based epidemic model. In section three we present the multi-scale computational protocol which can be used to efficiently detect coarse-grained bifurcations, while in section four we illustrate and discuss the results of our simulations; we detect the criticalities and we construct the coarse-grained bifurcation diagrams corresponding to two control policies as well as the one corresponding to the control-free dynamics. We conclude with the main outcomes of our work in section five.

II. THE MODEL

The epidemic evolves on a random regular graph [19], [20] which is characterized by a constant connectivity degree d between individuals. The graph is a caricature of the social structure of our artificial world involving N individuals. The states of the individuals change over discrete time in a probabilistic manner according to simple rules involving their own states and the states of their links. Each susceptible individual gets infected in a stochastic way with a probability depending on the number of its infected neighbors while the recovery probability varies nonlinearly with the number of the infected neighbors. Infected individuals can become isolated depending on the density of the infected population in the network.

More specifically each individual interacts with its links and changes its state, at every discrete time step t , according to the following rules:

Rule #1: An infected individual i infects a susceptible (S) neighbor j with a probability $p_{S \rightarrow I} = \lambda$, if an active link exists between them. This probability $p_{S \rightarrow I} \in [0, 1]$ expresses the infectivity degree of the disease.

Rule #2: An infected (I) individual withdraws him/herself with a probability $p_{I \rightarrow Q} = \rho$ and gets isolated (Q) from its links. Each isolated individual recovers with a probability $p_{Q \rightarrow R} = \delta$ at each time step. At each time step the transition from the state of infected to the state of isolation is determined by a function of the density of the infected

individuals in the network, say $[QI]$, where $[QI] = [I] + [Q]$. This function reflects the control policy of the spreading. Here we use two different types of control-isolation policies, namely a linear and a sigmoid one given by $p_{I \rightarrow Q} = [QI]$ and $p_{I \rightarrow Q} = \rho = \frac{1}{1 + e^{-12([QI]-0.5)}}$ respectively. Plots of these functions are given in Fig. 1.

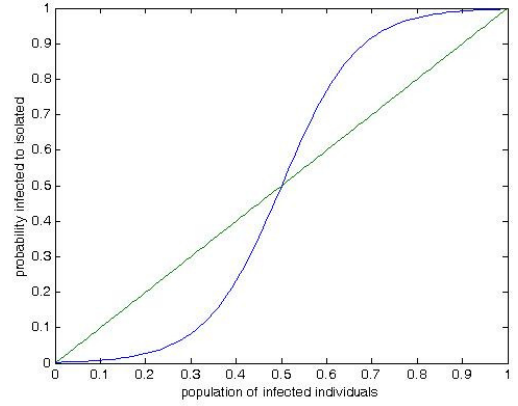


Fig. 1. Probability of an infected to become isolated. Two functions determine different control policies of isolation, i.e. the probability that an infected individual inactivates its links.

Rule #3: An infected individual recovers (R) with a probability $p_{I \rightarrow R} = \mu$. The probability of recovery depends nonlinearly on the number of infected links at time t , according to the function:

$$p_{I \rightarrow R} = \mu = \frac{y}{1 + e^{\frac{12(n(i)-0.5)}{d}}} + w, \text{ where } n(i) \text{ denotes the}$$

number of infected links of the infected individual i at time t , $(y+w)$ denotes the recovery probability of an infected individual with no infected links and w denotes the probability that an infected will recover even if all its links are also infected. Fig. 2 depicts $p_{I \rightarrow R}$ as a function of the infected links, for $y = 0.2$ and $w = 0.05$. At this point we should note that nonlinear incidence rates have been proposed in the literature to approximate in a better way the transmission mechanism of a disease spread. For example the authors in [4], [12] are using nonlinear incidence rates in the form of $k[I]^p[S]^q$ in a system of ordinary differential equations, trying to approximate the way the encounters among infected and susceptible individuals affect the transmission of the disease. Likewise, in [2], [6] nonlinear incidence rates were applied to networks of interacting individuals resulting to stable equilibrium solutions as well as periodic oscillations. Our relation depicts the fact that when the environment of an infected individual is “contaminated” it makes it more difficult to recover and thus the infection persists for a longer time. The nonlinearity may be accounted to different factors such as a drift of the

disease-virus over short time periods and heterogeneity in recovery [21].

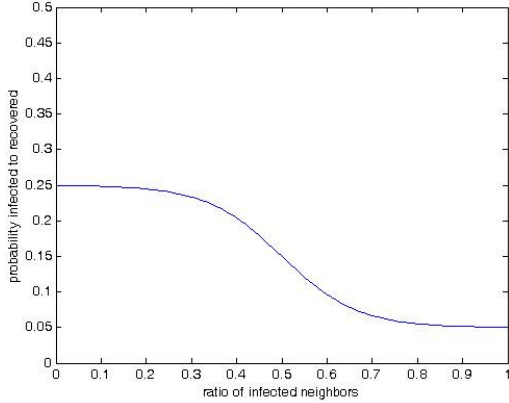


Fig. 2. The function defining the probability that an infected individual recovers as a function of the infected links.

Rule #4: A recovered individual becomes susceptible with a probability $p_{R \rightarrow S} = \varepsilon$. The condition of recovery is a state of temporal immunity: an individual who has suffered in the past acquires immunity for some time until it becomes vulnerable to the disease again.

Fig. 3 summarizes in a flow chart the rules governing the state transitions in our model.

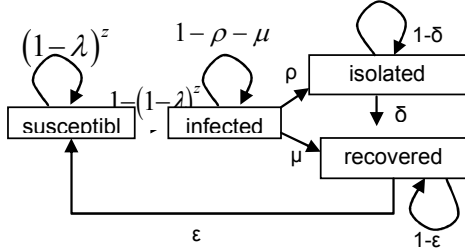


Fig. 3. Flow chart representing the transitions from one state to the others (z = number of infected neighbours with active links).

III. THE EQUATION-FREE PROTOCOL FOR DETECTING COARSE-GRAINED BIFURCATIONS

Our goal here is to develop a computational protocol that can enable detailed individual-based simulators to detect their coarse-grained bifurcation points. The method uses the Equation-Free computational concept which allows the systematic analysis of the dynamics of microscopic simulators circumventing the derivation of continuum closed-form equations [13]-[18]. The main assumption of the method is that a coarse-grained model for the individual-scale dynamics in principle exists and closes in terms of (relatively few) coarse-grained variables, but is overwhelming difficult or even impossible to derive. The dynamic detailed simulator is treated as a black-box input-output timestepper of the coarse-grained observables. In a nutshell, the black-box coarse timestepper is obtained through the following steps:

(1) Choose the coarse-grained statistics of interest for describing the long-term behavior of the system and an appropriate representation for them (for example the densities of the susceptible and infected individuals in the population).

(2) Choose an appropriate lifting operator μ from the continuum description \mathbf{u} to the individual-based description \mathbf{U} on the network. For example, μ could make random susceptible and infection assignments over the network consistent with the respective observed densities.

(3) Prescribe a continuum initial condition at a time t_k : \mathbf{u}_{t_k} .

(4) Transform this initial condition through lifting to one (or more) consistent individual-based realization(s) $\mathbf{U}_{t_k} = \mu \mathbf{u}_{t_k}$.

(5) Evolve thi(e)s realization(s) using the individual-based simulator for a desired time T , generating the $\mathbf{U}_{t_{k+1}}$, where $t_k = kT$.

(6) Obtain the restrictions $\mathbf{u}_{t_{k+1}} = \mathbf{M} \mathbf{U}_{t_{k+1}}$; lifting from the microscopic to the macroscopic and then restricting again should have theoretically no effect, that is, $\mathbf{M}\mu = \mathbf{I}$.

The above steps constitute the black-box coarse timestepper, that, given an initial coarse-grained state of the system $(\mathbf{u}_{t_k}, \mathbf{p})$ at time t_k reports the result of the integration of the individual-based rules after a given time-horizon T (at time $t_{k+1} = t_k + T$), i.e.

$$\mathbf{u}_{t_{k+1}} = \Phi_T(\mathbf{u}_{t_k}, \mathbf{p}) \quad (1)$$

where $\Phi_T: R^n \times R^m \rightarrow R^n$ having \mathbf{u}_k as initial condition; \mathbf{p} denotes the vector of the system parameters.

(7) Augment the fixed-point map equations $\mathbf{u} - \Phi_T(\mathbf{u}, \mathbf{p}) = \mathbf{0}$ by the appropriate condition with regard to the type of criticality sought and wrap around the augmented coarse map a computational superstructure such as simple Newton-Raphson or matrix-free iterative methods (quasi-Newton methods such as the Broyden, Fletcher, Goldfarb, Shanno (BFGS), direct methods such as the Nelder-Mead algorithm or Newton-GMRES) [22].

For a fold (or as otherwise called saddle-node) bifurcation and for $m=1$, the augmented system reads:

$$\begin{bmatrix} \mathbf{u} - \Phi_T(\mathbf{u}, \mathbf{p}) \\ (\mathbf{I} - \mathbf{J}(\mathbf{u}, \mathbf{p})) \mathbf{q} \\ \|\mathbf{q}\| = 1 \end{bmatrix} = \mathbf{0} \quad (2)$$

where $\mathbf{J}(\mathbf{u}, \mathbf{p}) \equiv \nabla_{\mathbf{x}} \Phi_T(\mathbf{u}, \mathbf{p})$ is the Jacobian matrix. The second equation in (2) implies that we seek critical points where the Jacobian is singular, a necessary condition for

fold bifurcations. Note that in the above formulation the explicit evaluation of the Jacobian is not required. Instead what is needed is the action of the Jacobian $\mathbf{J}(\mathbf{u}, \mathbf{p})$ on vectors, which can be obtained by calling the coarse black-box timestepper from appropriate nearby initial conditions and for the given time-horizon T .

For a Neimark-Sacker (a nondegenerate, two-dimensional) bifurcation the criticality condition reads [23]:

$$\mathcal{G}(\mathbf{u}, \mathbf{p}) \equiv \det[\mathbf{J}(\mathbf{u}, \mathbf{p})] - 1 = 0 \quad (3)$$

In this case the detection problem can be stated as a constrained minimization problem of the form

$$J = \min_{\mathbf{u} \in \mathbb{R}^m, \mathbf{p} \in \mathbb{R}} \left\{ \frac{1}{2} \mathcal{G}(\mathbf{u}, \mathbf{p})^2 \right\} \quad (4a)$$

subject to the constraints

$$\mathbf{u} - \Phi_T(\mathbf{u}, \mathbf{p}) = \mathbf{0} \quad (4b)$$

IV. SIMULATION RESULTS

For our illustrations we used the following values for the parameters: $N=20000$, $d = 4$, $p_{R \rightarrow S} = 0.4$, $y=0.2$, $w=0.05$. The two different control-policies are compared with the no-control (control-free) action where there is no isolation. We analysed the coarse-grained behaviour of the epidemic simulator by terms of the $p_{S \rightarrow I}$ which served as the bifurcation parameter. For our computations we used a cluster of 12 nodes running at 2.8 Ghz. All of our coarse-grained quantities have been extracted by averaging the temporal simulations after the transient, over 100 ensembles starting from the same coarse-grained initial conditions.

In the case where there is no isolation, i.e. no control action is deployed, the model is reduced to a Susceptible – Infected – Recovered – Susceptible (SIRS) one with a nonlinear recovery rate. Fig. 4 depicts the evolution of the infected population density for different values of the infectivity rate. Here the population density of infected individuals increases rapidly until it reaches a steady state for each value of the infectivity rate. Fig. 5 shows the corresponding coarse-grained bifurcation diagram with respect to the $p_{S \rightarrow I}$. As it can be easily seen, the disease dominates in the population even for small values of the infectivity rate and only for values less than $p_{S \rightarrow I} \sim 0.1$ the infected population is the minority. Around this value there is a dramatic change in the state of the network: for a small increment in $p_{S \rightarrow I}$ there is a big increase in the number of infected individuals reaching $\sim 60\%$ of the total population at $p_{S \rightarrow I} = 0.2$.

Fig. 6 shows a representative temporal simulation of one ensemble for the linear control policy at $p_{S \rightarrow I} = 0.7$. The density of infected individuals approaches fast a stationary

state. A similar behaviour is observed for all the values of the probability $p_{S \rightarrow I}$.

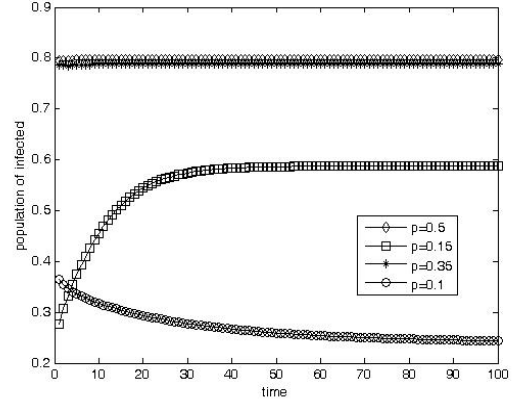


Fig. 4. Temporal coarse-grained simulations for the control-free case for $p_{S \rightarrow I} = 0.1, 0.15, 0.35$ and 0.5 .

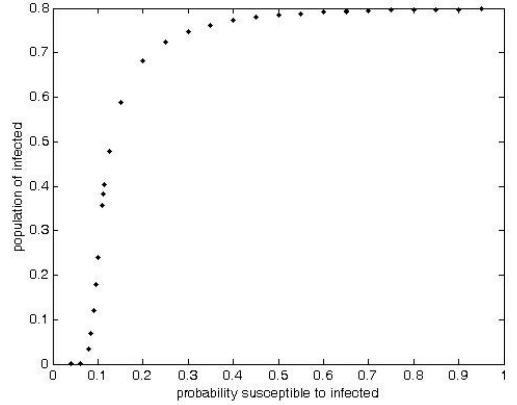


Fig. 5. Coarse-grained bifurcation diagram of the density of the infected population with respect to $p_{S \rightarrow I}$ for the control-free case.

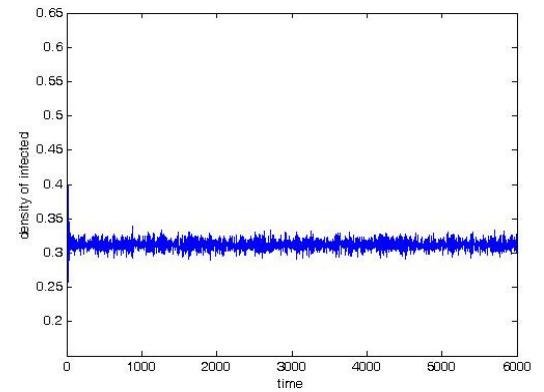


Fig. 6. Density of infected individuals in time. The probability of infection is 0.7 and the removal/isolation rate is the linear one.

Fig. 7 shows the corresponding coarse-grained bifurcation diagram depicting the density of the infected population with respect to $p_{S \rightarrow I}$. For very small values of the infection probability the only stable solution is the disease-free one. At a critical value around $p_{S \rightarrow I} = 0.09$ the disease-free state

looses stability through a transcritical bifurcation giving birth to a branch of endemic states, where the susceptible, infected and recovered individuals co-exist.

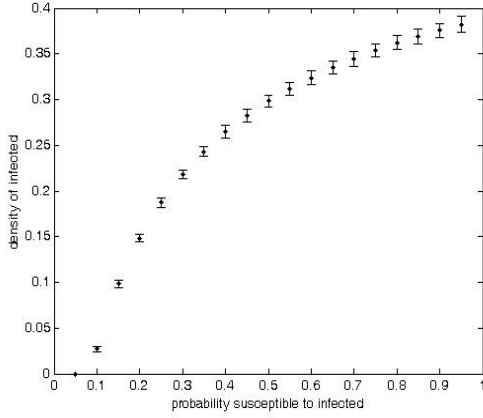


Fig. 7. Coarse-grained bifurcation diagram of the density of the infected population with respect to $p_{S \rightarrow I}$ using the linear control policy. Error estimates of the coarse-grained equilibria are depicted with bars.

Compared to the control-free case the linear control policy succeeds to remarkably reduce (or even extinguish for very small values of the $p_{S \rightarrow I}$) the percentage of the infected individuals into the population.

Some interesting nonlinear dynamics emerge when the sigmoid control policy is deployed: for relatively small values of the $p_{S \rightarrow I}$ the epidemic network follows a similar qualitative behaviour as in the linear control case leading to stationary states (Fig. 8). However as the $p_{S \rightarrow I}$ gets bigger the network gives rise to sustained periodic-oscillating solutions leading to periodic boom and bust outbreaks of the infection (Fig. 9a and 9c). The amplitudes increase with $p_{S \rightarrow I}$. Fig. 9 b and 9d depict the approximation of the power spectrum as obtained by applying a discrete fast fourier (FFT) transform algorithm on the corresponding time series. This reveals that the signal is periodic at a frequency around 0.08 Hz (an equivalent of 12 time steps).

This behavior indicates the existence of a Neimark-Sacker bifurcation whose exact location was derived using the proposed computational protocol. The time horizon was set to $T = 7$ time steps, while the number of ensembles was set to 4000. The algorithm used to solve the optimization problem was a quasi-Newton procedure [23]. The approach converged to the “correct” coarse-grained bifurcation point at $p_{S \rightarrow I} \sim 0.57$ as it also validated by the coarse-grained bifurcation diagram obtained by extensive temporal simulations (Fig. 10).

As expected, the branch of stable stationary solutions looses its stability at the critical point giving birth to a branch of stable coarse-grained limit cycles. As it is clearly seen the sigmoid control policy leads to epidemic oscillations of big-amplitudes, an undesirable phenomenon which can potentially drive the system to an-all-infected state.

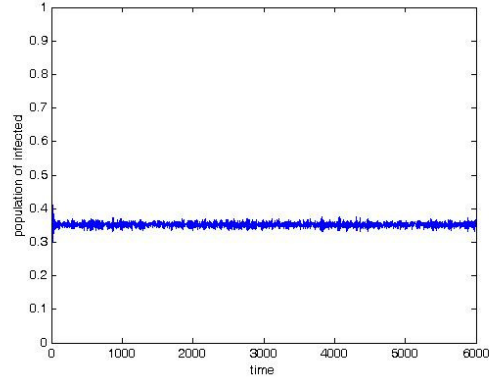


Fig. 8. Temporal simulations with the sigmoid control policy when the rate of infectivity is $p_{S \rightarrow I} = 0.3$.

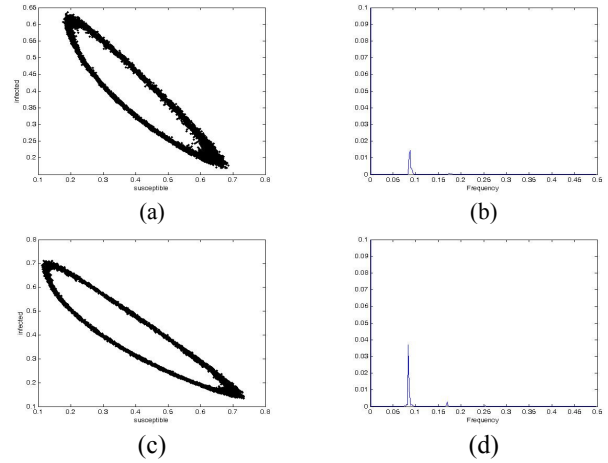


Fig. 9. (a) Phase diagram of the susceptible vs. the infected population density using the sigmoid control policy at $p_{S \rightarrow I} = 0.7$, (b) the corresponding power spectrum of the time series at $p_{S \rightarrow I} = 0.7$, (c) Phase diagram of the susceptible vs. the infected population density using the sigmoid control policy at $p_{S \rightarrow I} = 0.9$. (d) the power spectrum of the time series at $p_{S \rightarrow I} = 0.9$.

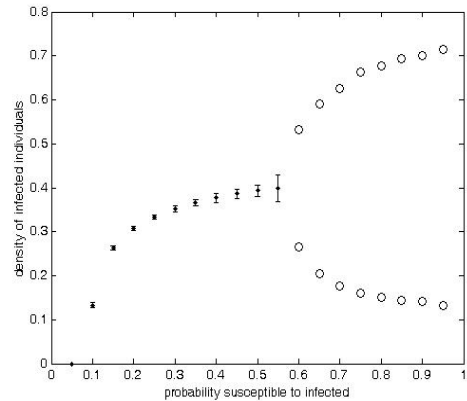


Fig. 10. The coarse-grained bifurcation diagram of the density of the infected population with respect to $p_{S \rightarrow I}$ using the sigmoid control policy. The circles depict the maximum and the minimum values of the oscillations.

V. CONCLUSION

The systematic investigation of the dynamics of fine-scaled epidemic simulators is of utmost importance in practical crisis management and control-intervention design policies. However for such detailed models, the closures required to formulate the problem in the continuum are usually not available and thus traditional numerical analysis and control design algorithms cannot be used. What is currently done with these state-of-the-art simulators is simple temporal simulation. Yet, simulation in time is but the first of systems level tasks one wants to do while analyzing the behaviour of a model. Important tasks such as the efficient exact location of criticalities which mark the onset of instabilities and undesirable phenomena such as big-amplitude sustained endemic oscillations cannot be easily obtained through just temporal simulations.

We presented a computational protocol based on the Equation-free framework for multi-scale computations to systematically study certain aspects of the dynamics of individual-based epidemic simulators. In particular we showed how the framework can be used to effectively detect critical points such as Neimark-Sacker bifurcations. This numerically motivated protocol may be much more practical and computationally efficient than simple simulation runs. The approach does not rely on the availability of closed-form continuum equations. Rather it treats the fine-scale simulator as a coarse timestepper to identify "on demand" the quantities that a numerical analysis algorithm would need evaluated from a macroscopic model, had such a model been available, to perform its task.

For our illustrations we developed an individual-based epidemic model with interactions deploying in a random regular network with nonlinear incidence rates. We considered isolation of the infected population as a control strategy against the transmission of the disease and we evaluated the impacts of two different approaches. A comparison of the infection dynamics with the control-free case is also illustrated. The proposed model, and depending on the chosen policy, exhibits some interesting nonlinear behavior such as sustained periodic oscillations.

Using the proposed multi-scale computational algorithm we effectively detected a Neimark-Sacker bifurcation which pinpoints the origin of the phenomena. To get a better understanding of the consequences related with the design of the control-policies we also constructed the coarse-grained bifurcation diagrams with respect to the parameter representing the transmission probability of the disease.

The analysis revealed that simpler strategies such as a linear dependence between the isolation rate and the percentage of the infected population, meaning action in the early stage of the epidemic can result in a better control of the spread. Delayed actions-which may be due to insufficient surveillance and response mechanisms-and a vast control effort at the late stages of the epidemic, as this is represented by the sigmoid dependence between the isolation rate and the

density of the infected population can give rise to undesirable phenomena such as big-amplitude sustained oscillations.

REFERENCES

- [1] M. J. Keeling, "The effects of local spatial structure on epidemiological invasions," *Proc. R. Soc. London*, vol. 266, pp. 859-867, 1999.
- [2] D. Greenhalgh, and P. Das, "Modelling epidemics with Variable Contact rates," *Theoretical Population Biology*, vol. 47, pp. 129-179, 1995.
- [3] H. Hethcote, M. Zhiem, and L. Shengbing, "Effects of Quarantine in six endemic models for infectious diseases," *Mathematical Biosciences*, vol. 180, pp. 141-160, 2002.
- [4] S. M. Moghadas, and M. E. Alexander, "Bifurcation of an epidemic model with non-linear incidence and infection-dependent removal rate," *Mathematical Medicine and Biology*, vol. 23, pp. 231-254, 2006.
- [5] W. Wang, and S. Ruan, "Bifurcations in an epidemic model with constant removal rate of the infectives," *J. Math. Anal.*, vol. 291, pp. 775-793, 2004.
- [6] T. Day, A. Park, N. Madras, A. Gumel, and J. Wu, "When is Quarantine a Useful Strategy for Emerging Infectious Diseases?," *Am. J. Epidemiol.*, vol. 163, pp. 479-485, 2006.
- [7] C. Fraser, S. Riley, R. M. Anderson, and N. M. Ferguson, "Factors that make an infectious disease outbreak controllable," *PNAS*, vol. 101, pp. 6146-6151, 2004.
- [8] R. M. Anderson, and R. M. May, "Population biology of infectious diseases," *Nature*, vol. 280, pp. 361-367, 1979.
- [9] F. Brauer, and C. Castillo-Chavez, *Mathematical models in population biology and epidemiology*. New York: Springer-Verlag, 2001.
- [10] N. M. Ferguson, D. A. T. Cummings, S. Cauchemez, C. Fraser, S. Riley, A. Meechai, S. Iamsrithaworn, and D. S. Burke, "Strategies for containing an emerging influenza pandemic in Southeast Asia," *Nature*, vol. 437, pp. 209-214, 2005.
- [11] I. M. Longini, P. E. Fine, and S. B. Thacker, "Predicting the global spread of new infectious agents," *Am. J. Epidemiol.*, vol. 123, pp. 383-91, 1986.
- [12] S. H. Eubank, V. S. A. Guclu, M. Kumar, M. V. Marathe, A. Srinivasan, Z. Toroczkai, and N. Wang, "Modelling disease outbreaks in realistic urban social networks," *Nature*, vol. 429, pp. 180-184, 2004.
- [13] I. G. Kevrekidis, C. W. Gear, J. M. Hyman, P. G. Kevrekidis, O. Runborg, and C. Theodoropoulos, "Equation-free coarse-grained multiscale computation: enabling microscopic simulators to perform system-level tasks," *Comm. Math. Sciences*, vol. 1, pp. 715-762, 2003.
- [14] A. Makeev, D. Maroudas, and I. G. Kevrekidis, "Coarse stability and bifurcation analysis using stochastic simulators: Kinetic Monte Carlo examples," *J. Chem. Physics*, vol. 116, pp. 10083-91, 2002.
- [15] C. I. Siettos, A. Armaou, A. G. Makeev, and I. G. Kevrekidis, "Microscopic/Stochastic timesteppers and Coarse Control: a kinetic Monte Carlo example," *AIChE J.*, vol. 49, pp. 1922-1926, 2003.
- [16] C. I. Siettos, M. Graham and I. G. Kevrekidis, "Coarse Brownian dynamics for nematic liquid crystals: bifurcation diagrams via stochastic simulation," *J. Chem. Physics*, vol. 118, pp.10149-156, 2003.
- [17] I. G. Kevrekidis, C. W. Gear, and G. Hummer, "Equation-free: the computer-assisted analysis of complex, multiscale systems," *AIChE J.*, vol. 50, pp. 1346-1354, 2004.
- [18] J. Chisternas, C. W. Gear, S. Levin, and I. G. Kevrekidis, "Equation-free modelling of evolving diseases: coarse-grained computations with individual-based models," *Proc. R. Soc. Lond. A*, vol. 460, pp. 1-19, 2004.
- [19] P. Erdos, and T. Gallai, "Graphs with prescribed degrees of vertices," *Mat. Lapok.*, vol. 11, pp. 264-274, 1960.
- [20] B. McKay, and N. Wormald, "Uniform generation of random regular graphs of moderate degrees," *J. Algorithms*, vol. 11, pp. 52-67, 1990.
- [21] M. Roy, and M. Pascual, "On representing network heterogeneities in the incidence rate of simple epidemic models," *Ecological Complexity*, vol. 3, pp. 80-90, 2006.

- [22] J. S. Anderson, S. Y. Shvartsman, G. Flätgen, and I. G. Kevrekidis, "Adaptive method for the experimental detection of instabilities," *Phys. Rev. Letters*, vol. 82, 532-535, 1999.
- [23] C. T. Kelley, *Iterative methods for linear and nonlinear equations*. Philadelphia: SIAM, 1995.